

Water and heat flow in a directionally frozen silty soil

K. Watanabe

Graduate School of Bioresources, Mie University, 1577 Kurima-Machiya, Tsu 514-8507, Japan

ABSTRACT: Directional freezing experiments on silty soil were carried out. The water and heat flows were calculated using the modified version of the HYDRUS-1D code, which includes a soil freezing model. In this model, the liquid water pressure at subzero temperatures was determined using temperatures, and the liquid (unfrozen) water content was estimated from soil water characteristic (retention curve) at room temperature. Unfrozen water content profiles can be simulated when proper temperature profiles are calculated. The model can also simulate water flow from the unfrozen region to the freezing front and the moisture profile in the unfrozen region. The calculated ice content roughly agreed with the column experiment when an impedance factor for the hydraulic conductivity was adjusted. However, water flow in the frozen region was not obtained since the impedance factor reduced the hydraulic conductivity too much. Better estimation of the hydraulic conductivity of frozen soils will be needed in future.

1 INTRODUCTION

In soil, some water remains unfrozen at subzero temperatures and the amount of unfrozen water decreases with the temperature. The relationship between the amount of unfrozen water, θ_l , and temperature, T , is called the soil freezing curve (SFC). Understanding how unfrozen water flows through frozen ground is important in investigations of water and solute redistribution (Baker & Spaans, 1997), soil microbial activity (Watanabe & Ito, 2008), mechanical stability and frost heaving (Wettlaufer & Worster, 2006), waste disposal (McCauley *et al.*, 2002), and climate change in permafrost areas (Lopez, 2007). To simulate the unfrozen water flow in unsaturated frozen soils, it is necessary to know not only how to express the hydraulic and thermal conductivities of the frozen soil but also how to determine its soil retention curve (soil water characteristics SWC; relationship between θ_l and the pressure head, h) and the SFC.

Williams (1964) and Koopmans & Miller (1966) measured the SFC and SWC of the same soils under freezing and drying processes and found a unique relationship between the negative temperature at which a given unfrozen water content occurs and the suction, corresponding to a similar moisture content at room temperature. Harlan (1973) derived the SFC from SWC using this relationship and analyzed the coupled heat and water flow in partially frozen soil numerically. In the Harlan's simulation, the unsaturated hydraulic conductivity of soil at room temperature was also applied to that of frozen soil, assuming the same pore water geometry for frozen and unfrozen soils. However, numerical simulations have suggested that this assumption overestimates water flow near the freezing front (Harlan, 1973; Taylor & Luthin, 1974; Jame & Norum, 1980). When the soil is frozen, the presence of ice in some pores may block water flow. To account for this blocking, several impedance factors have been introduced (*e.g.*, Jame & Norum, 1980; Lundin, 1990; Smirnova *et al.*, 2000). However, Black & Hardenberg (1991) criticized the use of an impedance factor, stating that it is a potent and wholly arbitrary correction function for determining the hydraulic conductivity of frozen soils. Newman & Wilson (1997) also concluded that an impedance factor is unnecessary when an accurate SWC and the relationship between hydraulic conductivity and water pressure are defined.

Harlan's concept and the impedance factor have been improved in several numerical studies (e.g., Flerchinger & Saxton, 1989; Zhao *et al.*, 1997; Stähli *et al.*, 1999). Hansson *et al.* (2004) also included these models in the HYDRUS-1D code and analyzed both laboratory and field soil-freezing experiments. In this study, we performed a laboratory directional freezing experiment of unsaturated silty soil and simulated movement of water and heat in the soil using the modified HYDRUS-1D code to verify the models with the impedance factor and to estimate the thermal and hydraulic conductivity of the frozen soil.

2 SOIL FREEZING MODEL

2.1 Water and heat flow equations

Assuming that vapor and ice flows are negligible, variably saturated water flow in above-freezing and subzero soil is described using a modified Richards' equation as follows (e.g., Noborio *et al.*, 1996; Hansson *et al.*, 2004):

$$\frac{\partial \theta_i(h)}{\partial t} + \frac{\rho_i}{\rho_l} \frac{\partial \theta_i(T)}{\partial t} = \frac{\partial}{\partial z} \left(K_h \frac{\partial h}{\partial z} + K_h + K_T \frac{\partial T}{\partial z} \right) \quad (1)$$

where θ_i is the volumetric ice content, t is time, z is the spatial coordinate, ρ_i is the density of ice, and K_h and K_T are the hydraulic conductivities of the flow due to a pressure head gradient and due to a temperature gradient, respectively. When ice is formed in soil pores, it releases latent heat, L_f , and the heat transport is described as follows:

$$C_p \frac{\partial T}{\partial t} - L_f \rho_i \frac{\partial \theta_i}{\partial t} = \frac{\partial}{\partial z} \left(\lambda \frac{\partial T}{\partial z} \right) - C_l q_l \frac{\partial T}{\partial z} \quad (2)$$

where C_p and C_l are the volumetric heat capacity of the soil particles and liquid water, respectively, λ is the thermal conductivity, and q_l is the liquid water flux. The left-hand side of equation (2) can be rewritten using the apparent volumetric heat capacity, C_a .

$$\left(C_p - L_f \rho_i \frac{\partial \theta_i}{\partial T} \right) \frac{\partial T}{\partial t} = \left(C_p + L_f \rho_i \frac{\partial \theta_i}{\partial T} \right) \frac{\partial T}{\partial t} = C_a \frac{\partial T}{\partial t} \quad (3)$$

Equations (1) and (2) are a tightly coupled duet due to their mutual dependence ofn the water content, pressure head, and temperature, and can be solved when the SWC and SFC are available.

2.2 Soil water pressure in a frozen soil

When ice and liquid water coexist, a state equation of phase equilibrium, known as a generalized form of the Clausius-Clapeyron equation (GCCE), arises.

$$v_l \frac{dP_l}{dT} - v_i \frac{dP_i}{dT} = \frac{L_f}{T} \quad (4)$$

where P_l and P_i are the liquid water and ice pressures, and v_l and v_i are the specific volumes of liquid water and ice, respectively. Assuming that GCCE is also valid in frozen soil with $P_l = \rho g h$ and $P_i = 0$, the matric potential of unfrozen water in frozen soil at an equilibrium state can be estimated from the temperature:

$$h = \frac{L_f}{g} \ln \frac{T}{T_m} \quad (5)$$

where T_m is the freezing temperature of bulk water in Kelvin.

When the soil pores illustrated in Figure 1a are filled with solute-free water and cooled below 0°C, water near the centers of the pores freezes easily, whereas water near the soil particles and at the corners among particles tends to remain in a liquid state due to the decrease in free energy resulting from surface and capillary forces. Further lowering of the temperature induces more ice formation, resulting in a decrease in the unfrozen water thickness with decreasing tempera-

ture. Williams (1964) and Koopmans & Miller (1966) regarded unfrozen water in freezing soil as having the same geometry as water in drying unsaturated soils (Fig. 1b), and assumed the same pressure difference between unfrozen water-ice interfaces and water-air interfaces. Under these assumptions, frozen soil at an h corresponding to the T from equation (5) contains the same amount of liquid water as unfrozen unsaturated soil at h ; that is the SFC can be estimated from the SWC. Furthermore, the slope of the SFC appearing in equation (3) is derived from the slope of SWC through GCCE:

$$\frac{d\theta_l}{dT} = \frac{d\theta_l}{dh} \frac{dh}{dT} = \frac{\rho g L_f}{v_w T} \frac{d\theta_l}{dh} \quad (6)$$

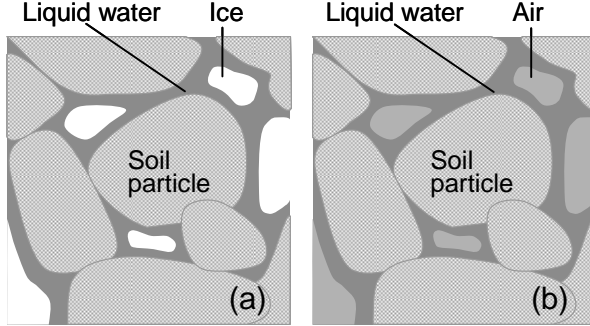


Fig. 1 Schematic illustration of liquid water geometry in soil pores: (a) freezing with the ice-liquid water interface in a saturated soil; (b) drying with the air-liquid water interface under room temperature.

2.3 Hydraulic and thermal properties

The water retention curve (SWC) and hydraulic conductivity, K_h , of unsaturated soil at room temperature are sometimes expressed using a formula proposed by Mualem (1976) and van Genuchten (1980):

$$S_e = \frac{\theta(h) - \theta_r}{\theta_s - \theta_r} = \left(1 + |\alpha h|^n\right)^{-m} \quad (7)$$

$$K_h = K_s S_e^l \left[1 - \left(1 - S_e^{1/m}\right)^m\right]^2 \quad (8)$$

where S_e is the effective saturation, θ_s and θ_r are the saturated and residual water content, respectively, K_s is the saturated hydraulic conductivity, and α , n , m , and l are empirical parameters. The soil water pressure at -1°C is estimated as $-12,500$ cm from equation (5), indicating that a SWC model that can express a relatively low pressure region is preferable for simulating frozen soil. For this purpose, in this study, we use the following equation, derived by Durner (1994), which combines two van Genuchten equations (7) using a weighting factor w :

$$S_e = w_1 \left[1 + (\alpha_1 h)^{n_1}\right]^{-m_1} + w_2 \left[1 + (\alpha_2 h)^{n_2}\right]^{-m_2} \quad (9)$$

$$K_h = K_s \frac{\left(w_1 S_{e1} + w_2 S_{e2}\right)^l \left(w_1 \alpha_1 \left[1 - \left(1 - S_{e1}^{1/m_1}\right)^{m_1}\right] + w_2 \alpha_2 \left[1 - \left(1 - S_{e2}^{1/m_2}\right)^{m_2}\right]\right)^2}{\left(w_1 \alpha_1 + w_2 \alpha_2\right)^2} \quad (10)$$

The hydraulic conductivity K_T for liquid water flow due to a temperature gradient is defined as (e.g., Hansson *et al.*, 2004):

$$K_T = K_{th} \left(hG \frac{1}{\gamma_0} \frac{d\gamma}{dT}\right) \quad (11)$$

where G is the enhanced factor, γ is the surface tension, and γ_0 is the tension at 25°C. If we assume the same liquid water geometry as shown in Figure 1, it is thought that the decrease in hydraulic conductivity of frozen soil with decreasing unfrozen water is also estimated by equation (8). However, several studies have reported that the use of the unsaturated hydraulic conductivity for unfrozen soil for frozen soil overestimates the water flow in frozen soil (*e.g.*, Jame & Norum, 1980; Lundin, 1990). Therefore, in this study, we invoke a modification of equation (8) using an impedance factor, Ω :

$$K_{fh} = 10^{-\Omega\theta_i/\phi} K_h \quad (12)$$

where ϕ is the porosity and θ_i/ϕ_T is the degree of ice saturation of the soil.

The soil heat capacity, C_p , can be estimated by summing the heat capacity, C , multiplied by the volumetric fraction, θ , of each soil element. With subscripts n , o , a , l , and i , for soil particles, soil organic matter, air, liquid water, and ice, respectively, and assuming that unfrozen water has the same heat capacity as liquid water at room temperature:

$$C_p = \theta_n C_n + \theta_o C_o + \theta_a C_{air} + \theta_l C_l + \theta_i C_i \quad (13)$$

Campbell (1985) introduced the relationship between the amount of liquid water and the thermal conductivity of soils, and Hansson *et al.* (2004) expanded this model to frozen soils by using the ice fraction parameter, F ,

$$\lambda = C_1 + C_2(\theta + F\theta_i) - (C_1 - C_4) \exp\left\{-[C_3(\theta + F\theta_i)]^{C_5}\right\} \quad (14)$$

$$F = 1 + F_1\theta_i^{F_2} \quad (15)$$

where C_1 ... C_5 , F_1 , and F_2 are empirical parameters.

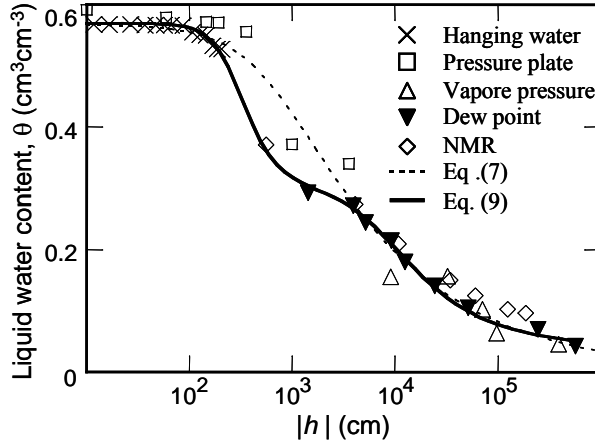


Fig. 2 Soil water characteristics of Fujinomori silt.

3 COLUMN FREEZING EXPERIMENT

3.1 Material and Methods

The samples used in this study consisted of Fujinomori silt, which is highly susceptible to frost and retains much liquid water, even when $T < -1^\circ\text{C}$. Figure 2 shows the SWC measured using several physical methods. Silt was mixed with water at $\theta = 0.4$ and packed at a bulk density of 1.18 into an acrylic column with an internal diameter of 7.8 cm and a height of 35 cm. Fifteen copper-constantan thermocouples and seven time domain reflectometry (TDR) probes were inserted into each column, and the side wall of the column was insulated. The TDR probes were initially calibrated for the measured unfrozen water content by comparison with a pulsed nuclear magnetic resonance (NMR) measurement. The column was allowed to settle at an ambient temperature of 2°C for 24 h to establish the initial water and temperature profiles and was then frozen from the upper end by controlling the temperature at both ends of the column ($T_L = -8^\circ\text{C}$

and $T_H = 2^\circ\text{C}$). During the experiment, no water flux was allowed from either end, and the profiles of temperature and water content were monitored using the thermocouples and TDR probes. A series of experiments with different durations of freezing was then performed for each freezing condition. At the end of the experimental series, the sample was cut into 2.5-cm sections to measure the total water content using the dry-oven method. The thermocouple and TDR readings confirmed that each column had the same temperature and water profiles during the series of experiments.

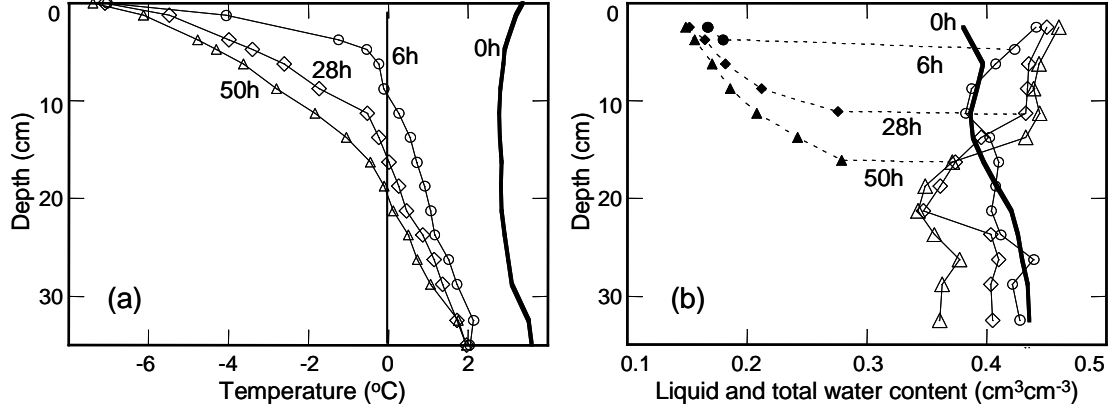


Fig 3. (a) Temperature and (b) moisture profiles measured in the frozen silt column (0, 6, 28, 50 h after freezing started). The solid line and dashed line in moisture profiles represent total water and unfrozen water contents, respectively.

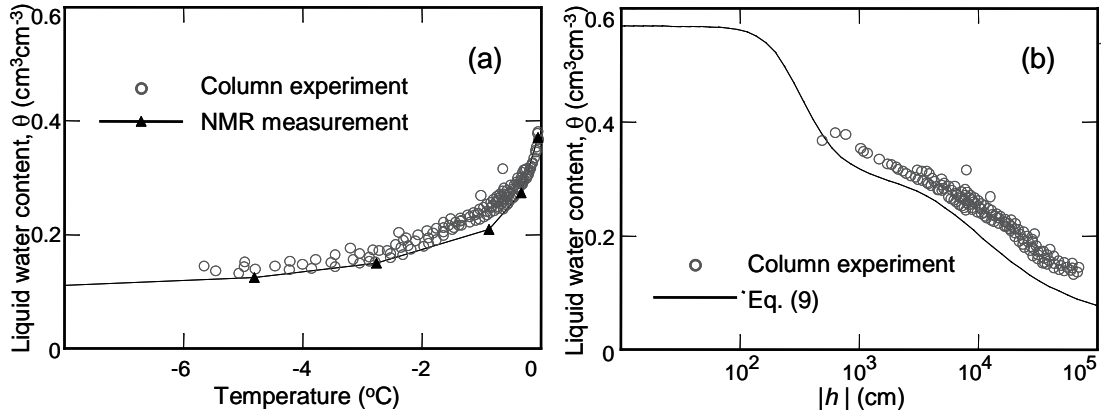


Fig. 4 (a) Soil freezing curve observed during the freezing experiment and measured by pulsed NMR methods under thermal equilibrium condition. (b) Soil water characteristics of Fujinomori silt estimated from (a).

3.2 Experimental results

Figure 3a shows the temperature profile of the freezing silt. When both ends of the column were set at different temperatures, the soil near the column ends reached the required temperatures quickly. The 0°C isotherm advanced at 1.57 , 0.34 , and 0.16 cm h^{-1} for 0–6, 6–24, and 24–48 h, respectively, and lowering of the freezing point by approximately 0.5°C was observed. The changes in the temperature profiles were smaller than expected from the thermal conductivity, implying heat flow from the side wall that prevented soil freezing. Although complete insulation was difficult in the laboratory experiment, the differences in the temperature and the location of the freezing front in soils at the center and near the wall of the column can be estimated within 0.5°C and to less than 1 cm, so we still regard it as directional freezing.

Figure 3b presents water profiles in silt at the same freezing times as shown in Figure 3a. The solid line indicates total water content, θ_T , measured using the dry-oven method, and the dashed line indicates the unfrozen water content, θ_i , measured using TDR. The ice content, θ_i , was obtained by subtracting the unfrozen water from the total water content. The silt had a relatively

vertical initial $\theta_l = \theta_T$ profile, having similar θ_l values for $h < 100$ cm (Fig. 2). An increase in θ_T , decrease in θ_l in the frozen area, and decrease in θ_l in the unfrozen area with the advancing freezing front were observed, implying that the soil water flowed not only through the unfrozen area but also through the frozen area.

Figure 4a shows the amount of unfrozen water measured with TDR during the freezing experiment (SFC). The amount of unfrozen water decreased sharply with temperature, although over $0.1 \text{ cm}^3 \text{ cm}^{-3}$ of water remained as a liquid at -8°C . Figure 4b compares the unfrozen water content as a function of the corresponding pressure based on equation (5) with the fitted SWC as shown in Figure 2. Since the frozen soil characteristics reasonably agreed with the unfrozen SWC well, we confirmed SWC can be applied as the frozen soil characteristics in the numerical simulation.

4 CALCULATIONS

The water and heat flows in the freezing experiment were simulated using a modified version of the HYDRUS-1D code. The measured temperature and water content (0 h in Fig. 3) in the 35-cm vertical silt column were given as the initial conditions. No water flux and a constant temperature ($T_{\text{top}} = -8^\circ\text{C}$ and $T_{\text{bottom}} = 2^\circ\text{C}$) were applied at both ends of the silt column for 48 h. No solute effect was considered in this simulation. Table 1 lists the hydraulic and thermal parameters used. From the fitted SWC (Figs. 2 and 4b) and measured saturated hydraulic conductivity, l in equation (10) was estimated with comparison to data from Watanabe & Wake (2008). The thermal conductivity of the frozen silt at different temperatures was first measured in the laboratory and the thermal parameters were estimated.

Table 1. Hydraulic and thermal parameter values for silt

θ_s	θ_r	α_1	n_1	α_2	n_2	w_2	K_s	l	θ_n	θ_o	C_1	C_2	C_3	C_4	F_1	F_2
m^3m^{-3}	m^3m^{-3}	m^{-1}		m^{-1}			m d^{-1}		m^3m^{-3}	m^3m^{-3}						
0.57	0.06	0.35	3.1	0.011	1.7	0.461	0.06	-0.08	0.55	0	0.72	0.84	8.38	0.093	13	1

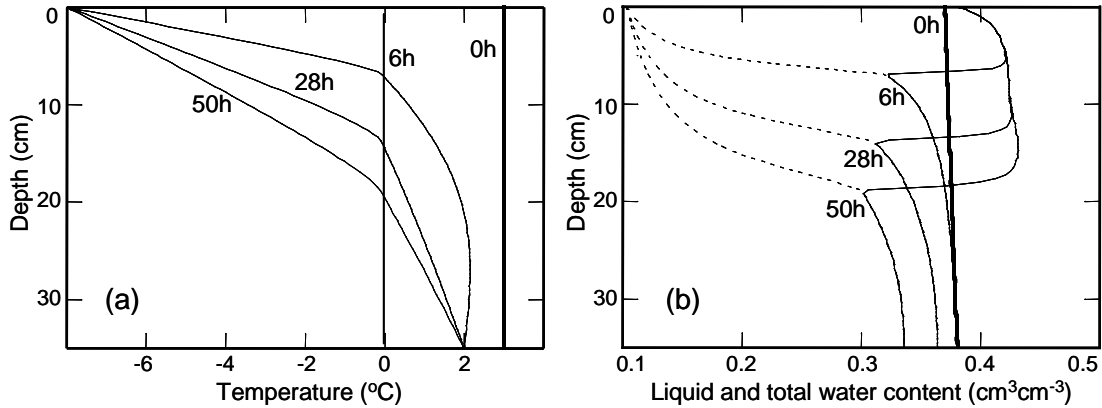


Fig. 5 Profiles of (a) temperature and (b) moisture in a directionally frozen silt calculated by using HYDRUS-1D code. The solid line and dashed line in moisture profiles represent total water and unfrozen water contents, respectively.

The calculated freezing rate underestimated the measured rate, since the heat flow from the side wall was not negligible in the laboratory experiment. Heat outflow through the wall causes quicker freezing than under fully insulated conditions, while inflow results in slower freezing. The calculated temperature profiles became congruent with the measured profiles (Fig. 5a) when the apparent thermal conductivity slightly larger than that obtained from the parameters in Table 1 was applied.

Figure 5b shows the water profile at this temperature profile. This model simulated the amounts of liquid water in both the frozen and unfrozen regions well, although the total amount of water in the frozen region was highly dependent on the impedance factor Ω (Fig. 6a). There

was a one-to-one relationship between temperature and the pressure of the unfrozen water in the frozen region. Therefore, the profile of the unfrozen water can be determined from the temperature profile directly, if the SFC is equivalent to the SWC. In other words, a reasonable unfrozen water profile can be obtained when proper temperature profiles are calculated. The water flow into and through the frozen soil appeared as a change in the total amount of water (or ice). When $\Omega = 0$, a huge pressure difference between the frozen and unfrozen regions induced water to flow to the freezing front, and the soil near the freezing front quickly reached ice saturation, so that water could no longer pass through it. Decreasing the hydraulic conductivity of frozen soil using Ω to reduce the water flow near the frozen front resulted in a decrease in the amount of ice near the frozen front; however, Ω cannot be evaluated from any soil properties and needs to be calibrated from the ice profile data itself. Furthermore, equation (12) provides an extremely small hydraulic conductivity for frozen soil according to Ω and the amount of ice (Fig. 6b) regardless of whether the amount of unfrozen water corresponds to the water path, and allows virtually no water flow in the frozen region (Fig. 5b, 6c, d). Further study of the hydraulic conductivity of frozen soil is needed to predict the total amount of water and water flow in frozen soil, which is important for estimating water balance, solute redistribution, gas emission, and snow water infiltration in cold regions.

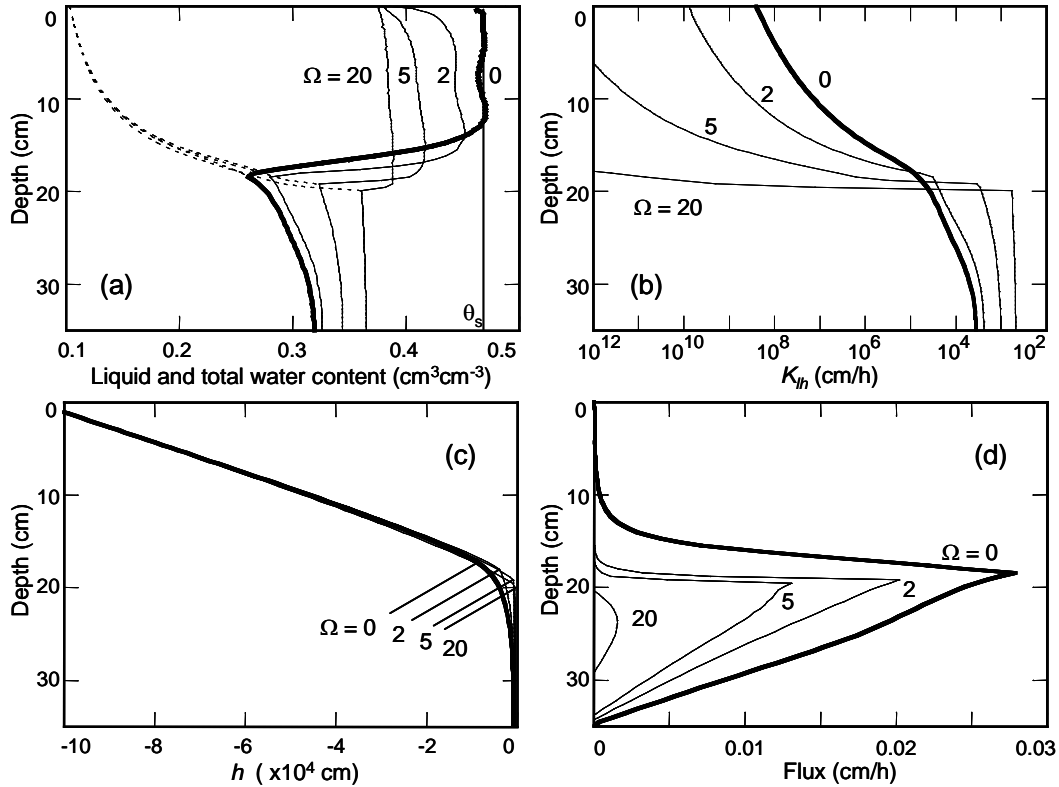


Fig.6 Profiles of (a) moisture, (b) hydraulic conductivity (c) pressure head, and (d) liquid water flux in a silt column which was directionally frozen 50 h, calculating with different impedance factor Ω .

5 SUMMARY

A freezing model for unsaturated frozen soil implemented in HYDRUS-1D could simulate water flow from the unfrozen region to the freezing front and the unfrozen water profile in the frozen region. It is very useful to consider the detailed mechanisms of water and heat flow in unsaturated soil under freezing conditions.

Since the impedance factor for the hydraulic conductivity is given as a function of ice water, it may underestimate the hydraulic conductivity as the ice water content increases. It would be necessary to describe the impedance factor in accordance with the unfrozen liquid water content instead of the ice content. Although the model assumed to reach the phase equilibrium instant-

neously, phase transition from liquid water to ice may take time to reach the equilibrium, and the transition rate would be proportional to the supercooling degree. If these time-dependent ice formations cannot be ignored, it is necessary to take into account for the non-equilibrium effects. As similar to the non-equilibrium flow and transport model, dual porosity or dual permeability formulation, for instance, may be also useful for the freezing model. Furthermore, solute concentration increases near the frozen front because of the solute exclusion, resulting in depression of freezing point of soil water. Future verification of these issues from both experiment and numerical simulation is important to evaluate water balance, solute redistribution, and snow melt infiltration in the frozen soil.

REFERENCES

- Baker, J. M. & Spaans, E. J. A. 1997. Mechanics of meltwater movement above and within frozen soil, Proc. Int. Sym. Physics, Chemistry, and Ecology of Seasonally Frozen Soils. CRREL Special Report, 97–10, pp. 31–36, US Army Cold Regions Research and Engineering Lab (CRREL), New Hampshire.
- Black, P. B. & Hardenberg, M. J. 1991. Historical perspectives in frost heave research, the early works of S. Taber and G. Beskow, CRREL Special Report, 91–23.
- Campbell, G.S. 1985. Soil physics with BASIC, Elsevier, New York.
- Dash, J. G., Fu, H. & Wettlaufer, J. S. The premelting of ice and its environmental consequences, *Rep. Prog. Phys.*, 58, 115–167.
- Durner, W. 1994. Hydraulic conductivity estimation for soils with heterogeneous pore structure. *Water Resour. Res.*, 30(2), 211–223.
- Flerchinger, G. N. & Saxton, K. E. 1989. Simultaneous heat and water model of a freezing snow-residue-soil system: I. Theory and development, *Trans. ASAE*, 32, 565–571.
- Hansson, K., Šimůnek, J., Mizoguchi, M., Lundin, L.-C. & van Genuchten, M. Th. 2004. Water flow and heat transport in frozen soil: Numerical solution and freeze-thaw applications, *Vadose Zone J.*, 3, 693–704.
- Harlan, R. L. 1973. Analysis of coupled heat-fluid transport in partially frozen soil, *Water Resour. Res.*, 9, 1314–1323.
- Jame, Y. W. & Norum, D. I. 1980. Heat and mass transfer in freezing unsaturated porous media, *Water Resour. Res.*, 16, 811–819.
- Koopmans, R. W. R., & Miller, R. D. 1966. Soil freezing and soil water characteristic curves, *Soil Sci. Soc. Am. Proc.*, 30, 680–685.
- Lopez, B. 2007. Cold Scapes, *National Geographic*, 212, 137–151.
- Lundin, L.-C. 1990. Hydraulic properties in an operational model of frozen soil, *J. Hydrolo.*, 118, 289–310.
- McCauley, C. A., White, D. M., Lilly, M. R. & Nyman, D. M. 2002. A comparison of hydraulic conductivities, permeabilities and infiltration rates in frozen and unfrozen soils, *Cold Regions Sci. Tech.*, 34, 117–125.
- Newman, G. P. & Wilson, G. W. 2004. Heat and mass transfer in unsaturated soils during freezing, *Can. Geotech. J.*, 34, 63–70.
- Smirnova, T. G., Brown, J. M., Benjamin, S. G. & Kim, D. 2000. Parameterization of cold-season processes in the MAPS land-surface scheme, *J. Geophys. Res.*, 105, 4077–4086.
- Stähli, M., Jansson, P.-E. & Lundin, L.-C. 1999. Soil moisture redistribution and infiltration in frozen sandy soils, *Water Resour. Res.*, 35, 95–103.
- Taylor, G. S. & Luthin, J. N. 1978. A model for coupled heat and moisture transfer during soil freezing. *Can Geotech. J.*, 15, 548–555.
- Watanabe, K & Ito, M. 2008. In situ observation of the distribution and activity of microorganisms in frozen soil, *Cold Regions Sci. Tech*, doi:10.1016/j.coldregions.2007.12.004.
- Wettlaufer, J. S., & Worster, M. G. 2006. Premelting dynamics, *Annu. Rev. Fluid. Mech.*, 38, 427–452.
- Williams, P. 1964. Unfrozen water content of frozen soil and soil moisture suction, *Geotechnique*, 14, 231–246.
- Zhao, L., Gray, D. M. & Male, D. H. 1997. Numerical analysis of simultaneous heat and mass transfer during infiltration into frozen ground, *J. Hydrol.*, 200, 345–363.